

# The Kemp elimination in membrane mimetic reaction media. Probing catalytic properties of cationic vesicles formed from a double-tailed amphiphile and linear long-tailed alcohols or alkyl pyranosides †

Jaap E. Klijn and Jan B. F. N. Engberts\*

Physical Organic Chemistry Unit, Stratingh Institute, University of Groningen, Nijenborgh 4, 9747 AG Groningen, The Netherlands

Received 3rd March 2004, Accepted 29th April 2004

First published as an Advance Article on the web 26th May 2004

Vesicles formed from synthetic, double-tailed amphiphiles are often used as mimics for biological membranes. However, biological membranes are a complex mixture of various compounds. In the present paper we describe a first attempt to study the importance of additives on vesicular catalysis. The rate-determining deprotonation of 5-nitrobenzoxazole (Kemp elimination) by hydroxide ion is efficiently catalysed by vesicles formed from dimethyldi-*n*-octadecylammonium chloride ( $C_{18}C_{18}^+$ ) as a result of (partial) dehydration of the reactants (especially the hydroxide ion) at the vesicular binding sites. Gradual addition of linear alcohols, such as *n*-decanol ( $C_{10}OH$ ), *n*-octadecanol ( $C_{18}OH$ ) and batyl alcohol ( $C_{18}GlyOH$ ) leads to a decrease in the observed catalysis. By contrast, gradual addition of oleyl alcohol, *n*-dodecyl- $\beta$ -glucoside ( $C_{12}Glu$ ) and *n*-dodecyl- $\beta$ -maltoside ( $C_{12}Mal$ ) leads to an increase in the observed catalysis. A detailed kinetic analysis, taking into account substrate binding site polarities, counterion binding percentages and binding affinity of the kinetic probe, suggests that the catalytic changes depend strongly on subtle changes in the structure of the additive. Whereas the  $C_{12}Glu$ -induced effect can be explained by an increase in the vesicular rate constant, the effect of  $C_{12}Mal$  can only be explained by an increase in the binding constant of the kinetic probe. However, for these pyranoside-containing vesicles other factors, such as a more extensive dehydration of the hydroxide ion, and micelle formation have to be considered. For the linear alcohols, besides a decrease in the counterion binding, changes in the vesicular rate constant and the binding constant should be taken into account. These two parameters change to a different extent for the different alcohols. The kinetic analysis is supported by differential scanning calorimetry (DSC),  $E_T(30)$  absorbance data and Nile Red, Laurdan, ANS and pyrene fluorescence measurements.

The overall kinetic results are illustrative for the highly complex mix of factors which determines catalytic effects on reactions occurring in biological cell membranes.

## Introduction

Micelles have been extensively studied with respect to their catalytic properties towards a variety of organic reactions.<sup>1–4</sup> Studies on vesicular catalysis<sup>5–8</sup> have been less frequent and are generally more complex since, contrary to micelles, vesicles are usually not thermodynamically stable and experiments yield more scattering in the data.

In general, two effects lead to catalysis of bimolecular reactions in micellar and vesicular aggregates.<sup>2</sup> The first effect comes from substrate–aggregate binding. Charged micelles and vesicles provide a good environment for hydrophobic and oppositely charged molecules to bind, thereby increasing the chances of two substrates to meet and react because the effective reaction volume is reduced. Particularly when one of the two reactants can bind as a counterion to the aggregate, efficient catalysis is found. The second effect comes from the modified reaction environment after binding of both reactants to the surfactant aggregate.

In the past 20 years reactions between counterions and organic substrates have been extensively studied in micelles with and without additives such as low molecular weight alcohols and/or alkanes,<sup>9–19</sup> or non-ionic cosurfactants.<sup>20–24</sup> To our knowledge no catalytic studies have been performed with

vesicles in the presence of additives, such as linear alcohols or alkyl pyranosides.

Vesicles can be used as mimics for aspects of the chemistry of the much more complicated biological membranes. The structural diversity of lipid molecules in biomembranes is very large and consists of over 1000 different structures. These structural differences are not only expressed in the head group, but also by a large variety in hydrophobic tails and in the linker between head group and tails.<sup>25,26</sup> Selective degradation of lipids plays an important role in signalling as second messenger or bioregulator. For example, in the brain phospholipase A<sub>1</sub>, A<sub>2</sub>, C and D generate among other molecules *sn*-1,2-diacylglycerol as second messenger.<sup>27</sup> In addition, during every one or two cell divisions half of the phospholipids have been degraded in order to maintain cell viability.<sup>28</sup> Therefore in most cell membranes it is very likely that several different alcohols are present to a certain extent.

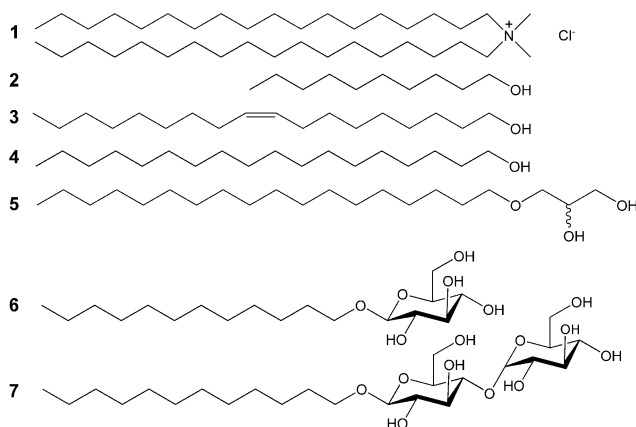
A special class of alcohols are the (synthetic) alkyl pyranosides.<sup>29</sup> Nature makes abundant use of these types of sugar amphiphiles (glycolipid; GL). Instead of a PC or PE moiety, an oligosaccharide acts as the head group. The outer leaflet of almost all animal cell plasma membranes contains up to ca. 25% of glycolipids.<sup>30</sup> Therefore it is believed that GLs play an important role in the interaction of cells with their environment. Especially since there are many possible structures, there can be a large variety of functions. For example, GLs can act as receptor for recognition or as protection against harsh conditions (low pH, degradative enzymes). Also dehydration of the

† Electronic supplementary information (ESI) available: Further experimental details and figures. See <http://www.rsc.org/suppdata/ob/b4/b403237c/>

interfacial region might become important at high local GL content.<sup>31</sup>

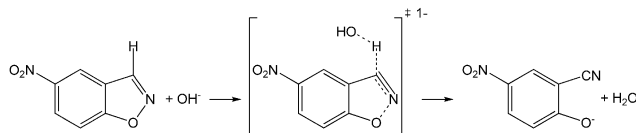
In recent years it has been found that synthetic nonionic sugar-based amphiphiles are able to “adsorb” hydroxide ions.<sup>32–36</sup> However, the adsorption mechanism has not yet been revealed, although the structure of the first hydration shell of the polar–apolar interface might be important.<sup>37</sup> The adsorption of hydroxide ions has not yet been observed in biological (GL containing) membranes.

Based on the above-mentioned properties of linear alcohols and GLs we decided to exploit the catalytic properties of cationic vesicles formed from dimethyldi-*n*-octadecylammonium chloride ( $C_{18}C_{18}^+$ ) in the presence of linear alcohols (Scheme 1). *n*-Decanol ( $C_{10}OH$ ) and *n*-octadecanol ( $C_{18}OH$ ) were selected since they have a considerable mismatch and match, respectively, with the chain length of the amphiphile. Oleyl alcohol ( $C_{18:1}OH$ ) and batyl alcohol ( $C_{18}GlyOH$ ) were chosen in order to study the influence of the unsaturation in the tail and of the presence of additional hydroxyl groups, respectively. Two synthetic alkyl pyranosides were chosen: *n*-dodecyl- $\beta$ -glucoside ( $C_{12}Glu$ ) and *n*-dodecyl- $\beta$ -maltoside ( $C_{12}Mal$ ). The first is a monosaccharide, the second a disaccharide. These additives were selected not so much to mimic the overall properties of cell membranes, but rather in an attempt to identify the factors that play a role in determining the properties of cell membranes as reaction media.



**Scheme 1**  $C_{18}C_{18}^+$  (1);  $C_{10}OH$  (2);  $C_{18:1}OH$  (3);  $C_{18}OH$  (4);  $C_{18}GlyOH$  (5);  $C_{12}Glu$  (6);  $C_{12}Mal$  (7).

The bimolecular base-catalysed deprotonation reaction of 5-nitrobenzisoxazole (Scheme 2) has been studied in some detail.<sup>38</sup> The reaction is sensitive to the local reaction environment and the local hydroxide-ion concentration. In apolar environments the second-order rate constant is much higher than in polar environments. This makes it an ideal kinetic probe reaction to study the influence of the alcohols and pyranosides mentioned above. In a previous paper we have shown its sensitivity towards the addition of negatively charged amphiphiles to cationic vesicles.<sup>8</sup>



**Scheme 2** Kemp elimination reaction.

## Results and discussion

### Outline

In this section we will first describe the effects of the structure and mole fraction of the various additives on the observed rate constants of the cationic-vesicle catalysed Kemp elimination reaction. Then the equations used to fit the observed rate

constants will be introduced. Particular attention is paid to parameter compensation. Subsequently, different methods of fitting the experimental data are discussed, and the data is fitted using the most appropriate method. For clarity of the discussion of the effects of the additives on the fitted parameters, the additives are divided into two groups: (1) mono- and dihydric alcohols and (2) polyhydric alcohols (pyranosides). The trends in the fitted parameters are compared with literature observations. The possibility of specific or preferential binding of hydroxide ions to cationic vesicles containing the polyhydric alcohols is examined. Differential scanning microcalorimetry (DSC) is used to study the phase of the tails. In order to quantify the sensitivity of the rate constant as a function of the local polarity at the vesicular binding sites, rate constants in mixtures of water and organic solvents have been measured. Then, changes in membrane polarity are addressed using five different dyes that are sensitive towards changes in polarity. Finally, the results of the various techniques are combined and discussed.

### Vesicular catalysis

Cationic vesicles formed from dimethyldi-*n*-octadecylammonium chloride ( $C_{18}C_{18}^+$ ) efficiently catalyse the Kemp elimination reaction.<sup>8</sup> At 15 °C and in the presence of 2.25 mM NaOH the observed catalysis (ratio of the maximum observed rate constant to the observed rate constant in water) amounts to *ca.* 1000. A more detailed kinetic analysis, taking into account the distribution of the kinetic probe over the aqueous and vesicular phase and the vesicular reaction volume (*vide infra*), revealed that the bimolecular vesicular rate constant is about 50 times higher than the bimolecular aqueous rate constant. The 50-fold increase in rate constant upon binding to the vesicular surface is largely a result of reduced hydration of the hydroxide ion.<sup>39–41</sup> Both the initial state and transition state are destabilised, but due to the charge delocalisation in the transition state to a smaller extent relative to the initial state. Hence the rate constant increases.

The addition of up to 66 mol% of saturated linear alcohols, like  $C_{10}OH$ ,  $C_{18}OH$  and  $C_{18}GlyOH$ , to vesicles of  $C_{18}C_{18}^+$  leads in all ratios to a *decrease* in the catalysis by these membranes (Fig. 1A–C). However, the extent of the decrease depends on both the length of the tail and the nature of the “head group”, although the effect of the tail is more important. For example, addition of 50 mol% of  $C_{10}OH$  leads to a modest decrease of 8% in the maximum observed rate constant whereas addition of 50 mol% of  $C_{18}OH$  and  $C_{18}GlyOH$  leads to a lowering with 62% and 36%, respectively. Strikingly, the addition of 35 mol% of  $C_{18:1}OH$  leads to an *increase* of the maximum observed rate constant by 140% (Fig. 1D). An even stronger catalysis is found when  $C_{12}Mal$  or  $C_{12}Glu$  are present in 50 mol% in the membrane, since their presence leads to an increase in the maximum observed rate constant by a factor of 400% and 700% (Fig. 1E and F), respectively.

The observed rate constants for 20 mol% of  $C_{18}OH$  are higher than those for 10 mol% of  $C_{18}OH$ . This result is odd, but reproducible. We speculate that it might be related to a different packing at 20 mol% of  $C_{18}OH$  compared to 10 mol%.

### Kinetic analysis

The observed rate constants were analysed using a slightly modified version of the pseudophase model with ion exchange developed by Menger<sup>9</sup> and Romsted<sup>42</sup> and which we used in a previous study on the catalytic efficiency of  $C_{18}C_{18}^+$  mixed with an anionic co-amphiphile.<sup>8</sup> Since we have in the present study no charge compensation we can rewrite the previously used equations to afford eqns. (1) and (2).

$$k_{\text{obs}} = \frac{k_w[\text{OH}^-]_{\text{tot}} + (k_{\text{ves}}K_S - k_w)m_{\text{OH}}[C_{18}C_{18}^+]}{1 + K_S[\text{amph}]_{\text{tot}}} \quad (1)$$

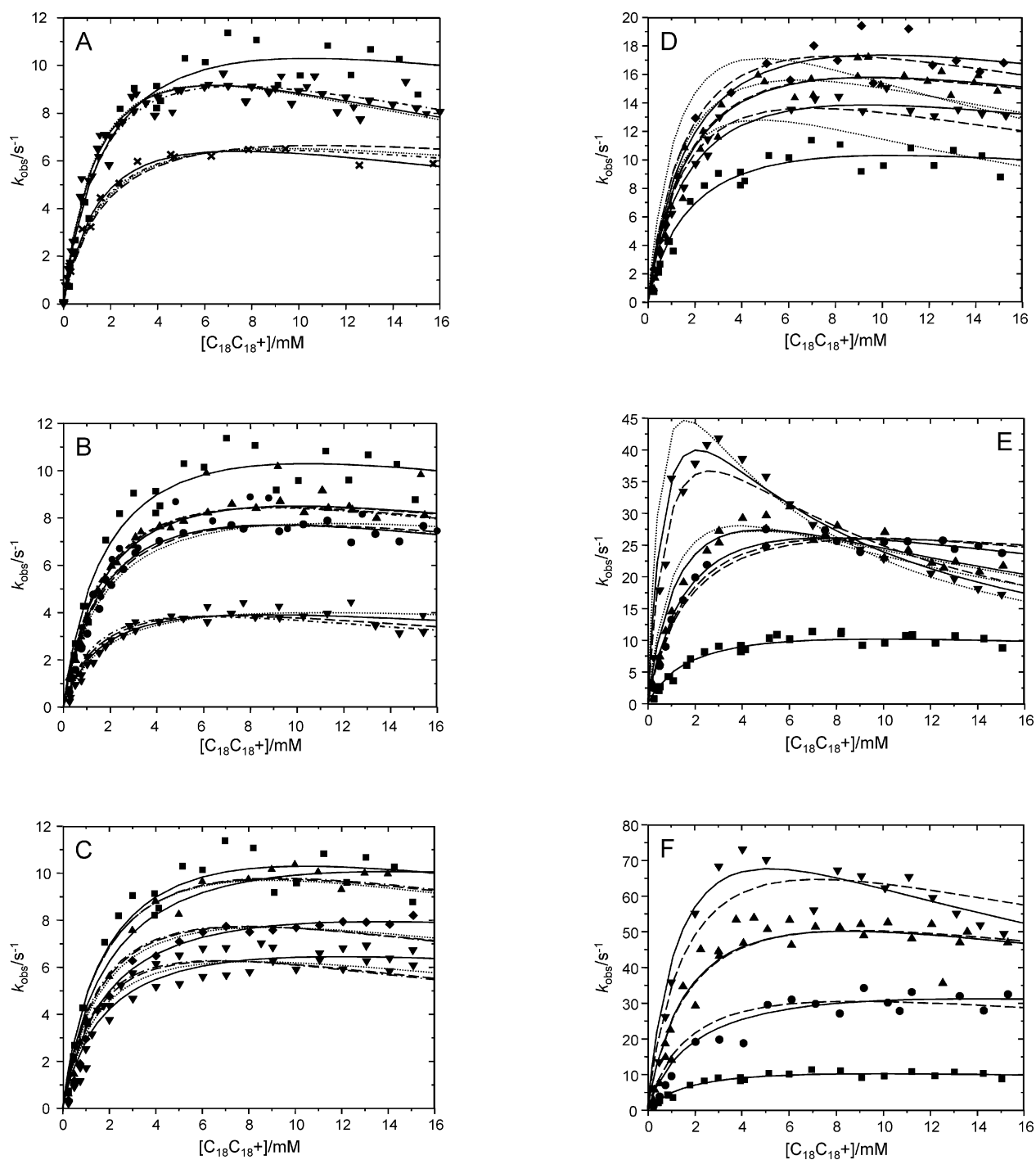


**Fig. 1** Kinetic curves for  $C_{18}C_{18}^+$  vesicles with  $C_{10}OH$  (A),  $C_{18}OH$  (B),  $C_{18}GlyOH$  (C),  $C_{18:1}OH$  (D),  $C_{12}Mal$  (E) and  $C_{12}Glu$  (F), where the additive is present in 0 mol% ( $\blacksquare$ ), 10 mol% ( $\bullet$ ), 20 mol% ( $\blacktriangle$ ), 35 mol% ( $\blacklozenge$ ), 50 mol% ( $\blacktriangledown$ ) and 66 mol% ( $\times$ ).  $C_{12}Mal$  and  $C_{12}Glu$  are not present in 20 mol%, but in 25 mol% ( $\blacktriangle$ ). Solid lines are fits allowing  $k_{ves}$  and  $K_S$  to vary, dotted lines are fits allowing  $K_S$  to vary, dashed lines are fits allowing  $k_{ves}$  to vary and dash-dotted lines are fits allowing  $\beta$  to vary. In A to D  $\beta$  was varied as described in the text.

$$m_{OH}^2 + m_{OH} \left[ \frac{[OH^-]_{tot} + K_{OH}^{Cl}[Cl^-]_{tot} + \beta}{(K_{OH}^{Cl} - 1)[C_{18}C_{18}^+]} \right] - \left[ \frac{\beta[OH^-]_{tot}}{(K_{OH}^{Cl} - 1)[C_{18}C_{18}^+]} \right] = 0 \quad (2)$$

In these equations  $k_{obs}$ ,  $k_w$  and  $k_{ves}$  are the observed, aqueous and vesicular rate constant, respectively.  $K_S$  is the binding constant of the kinetic probe to the bilayer (amphiphile and additives).  $K_{OH}^{Cl}$  is the exchange constant for binding of hydroxide and chloride ions to the bilayer and  $\beta$  is the total counterion binding to the bilayers.  $[OH^-]_{tot}$  is the total hydroxide ion concentration and  $m_{OH}$  is the ratio of concentrations of bound hydroxide ions and cationic amphiphiles.

$[C_{18}C_{18}^+]$  and  $[amph]_{tot}$  are the concentration of  $C_{18}C_{18}^+$  and the concentration of  $C_{18}C_{18}^+$  plus the concentration of additive, respectively.

The binding constant of the kinetic probe is given by eqn. (3). In this equation  $[P]_{ves}$  and  $[P]_w$  are the concentration of kinetic probe in the vesicular and aqueous pseudophase, respectively.

$$K_S = \frac{[P]_{ves}}{[P]_w [amph]_{tot}} \quad (3)$$

In eqns. (1) and (2) there are four parameters that are, in principle, unknown ( $k_{ves}$ ,  $K_S$ ,  $K_{OH}^{Cl}$  and  $\beta$ ). However, in the literature one can usually find reasonable values for these parameters when systems are involved that only contain a few

well-studied components (e.g. water and amphiphiles). In the case of a more complex mixture the data analysis becomes more difficult. If one compares two of these kinetic curves with each other it is usually possible to fit both curves reasonably well by adjusting just *randomly one* of the four parameters. This means that although the parameters have different physical meaning they compensate each other to a large extent.<sup>43–48</sup>

In order to get a better insight into the meaning of the fitted values of the parameters we calculated the error in these parameters by calculating  $\chi^2$ .

$$\chi^2 = \sum_{i=1}^{i=n} \frac{(k_{\text{calc}}^i - k_{\text{obs}}^i)^2}{(\sigma_{k_{\text{obs}}^i}^i)^2} \quad (4)$$

In this equation  $n$  is the number of data points,  $k_{\text{calc}}^i$  the calculated rate constant for the  $i^{\text{th}}$  data point and  $\sigma_{k_{\text{obs}}^i}^i$  is the estimated experimental error for that data point. If now one parameter in eqn. (1) or (2) is systematically slightly varied, and  $\chi^2$  is minimised by allowing a second parameter to vary, one obtains a new value for  $\chi^2$ . If for a certain variation in the systematically varied parameter, the new value of  $\chi^2$  is exactly equal to the original value then the parameter that was allowed to vary can perfectly compensate the parameter that was systematically varied. If the new value of  $\chi^2$  is just slightly higher, then the second parameter can just partially compensate the first parameter. In an ideal case the new value of  $\chi^2$  is much larger than the original value and then parameter compensation is nearly absent.

By systematically changing one parameter the parabola as shown in Fig. 2 is obtained and hence the error as a function of another parameter can be calculated by calculating the width of the parabola at a value of  $\chi^2 + 1$ . In this way the error in a parameter can be calculated as a function of any other parameter in the equations. The  $\chi^2$  values do not necessarily form a parabola, but usually this is quite a reasonable approximation.

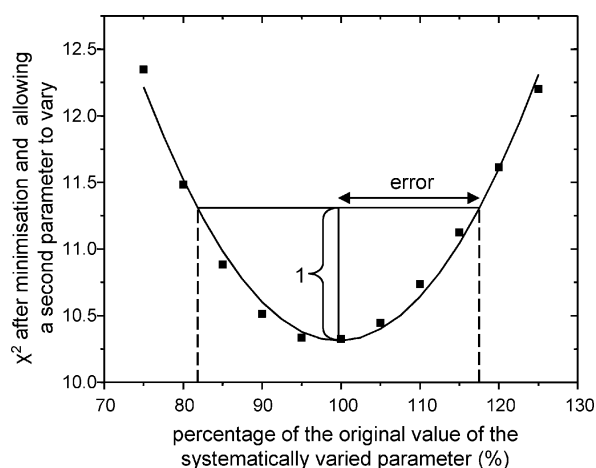


**Fig. 2** Example of calculating the error of a parameter as a function of another parameter (50 mol% of  $C_{18}\text{OH}$ ).

As can be seen in Table 1 the mutual dependence of the different parameters is in certain cases quite large. This problem has been observed before<sup>43,45–48</sup> and indicates that for this model, parameter compensation is quite significant. For example, an increase in  $k_{\text{ves}}$  can be quite well compensated by a decrease in counterion binding, since the error in this case is 42%. Likewise a change in  $K_S$  or  $\beta$ , respectively, can be compensated by changes in  $k_{\text{ves}}$  (27% and 32%). In this analysis the absolute error depends on the experimental error. If the experimental error is twice as small, the absolute errors will be twice as well, but the dependence of the parameters on each other is *not* affected. In our example of the addition of 50 mol%

**Table 1** Errors in the parameters as a function of the other parameters for 50 mol% of  $C_{18}\text{OH}$

	Value	Error $_{k_{\text{ves}}}$	Error $_{K_S}$	Error $_{\beta}$
$k_{\text{ves}}$	240	—	46 (19%)	101 (42%)
$K_S$	16.8	4.6 (27%)	—	3.0 (18%)
$\beta$	0.81	0.26 (32%)	0.10 (12%)	—

of  $C_{18}\text{OH}$  we estimated the experimental error to be  $0.5 \text{ s}^{-1}$  for all data points (except for the first three data points where the error was estimated to be 1). Most data points are within  $0.5 \text{ s}^{-1}$  from the fitted curve justifying our choice of  $0.5 \text{ s}^{-1}$ .

Considering both the parameter compensation and the complexity of the solution, we decided to fit the data in four different ways. In the first case (method I) we fixed  $K_{\text{OH}}^{\text{Cl}}$ ,  $k_{\text{ves}}$  and  $K_S$  as for 100%  $C_{18}\text{C}_{18}^+$  and allowed  $\beta$  to vary. In the other cases (method II, III and IV)  $\beta$  was systematically changed assuming that four alcohol molecules have the same area as one molecule  $C_{10}\text{C}_{10}^-$  (sodium didecylphosphate<sup>8</sup>) and one molecule  $C_{18}\text{C}_{18}^+$ . In vesicles composed of these two amphiphiles these two molecules form a neutral (catanionic) area in the bilayer, thereby causing a decrease in the local charge density and therefore leading to a decrease in the excess counterion binding.<sup>8</sup> This approach leads, for example, to a counterion binding of 0.77 when 50% alcohol is added to cationic vesicles. In method II  $K_S$  was varied, in method III  $k_{\text{ves}}$  was varied, and in method IV both  $k_{\text{ves}}$  and  $K_S$  were varied. The ion exchange constant was fixed at 1.6 and not expected to change, in agreement with literature data and our own observations (supplementary information †).<sup>18</sup> In Fig. 1A and B it can be seen that these different approaches do not lead to substantially different fits of the data, although in general method IV seems to give slightly better fits. However, it should be stressed that the values of the different parameters are quite different for the different fits.

In Fig. 1C and D the difference in fits for the different methods is larger. The data of vesicles with  $C_{18:1}\text{OH}$  could not be fitted with method I, since this would lead to a  $\beta$  larger than 1. Method II gives only bad fits, but method III gives fits that are acceptable. Much better agreement is obtained with method IV. For  $C_{18}\text{GlyOH}$  with methods I–III acceptable fits are found, whereas method IV gives a good fit with the experimental data.

In the case of the pyranosides it is interesting to note that the maximum observed rate constants are 4 (50 mol% of  $C_{12}\text{Mal}$ ) and 7 (50 mol% of  $C_{12}\text{Glu}$ ) times higher than in the absence of the pyranosides. In addition, the differences between the fitting methods are much clearer (Fig. 1E and F). For  $C_{12}\text{Mal}$  and  $C_{12}\text{Glu}$  the curves could not be fitted with method I since this would require a counterion binding larger than 1. Method III gives poor fits, whereas the best fits were obtained with method IV. For 10 mol% and 26 mol% of  $C_{12}\text{Glu}$  method III and IV give similar results, whereas for 50 mol% only method IV can fit the data satisfactorily.

In Fig. 3A and B the fitted parameters are shown for the best fits (method IV), and only these fits will be discussed here. The results for method II and III will not be discussed since the differences between the *methods* are too small to allow a meaningful interpretation. However, the differences between vesicles with and without added alcohol are significant.

The difference between  $C_{10}\text{OH}$  and  $C_{18}\text{OH}$  is particularly remarkable. The vesicular rate constants of both series do not change to a large extent, but the binding constant of the kinetic probe moves in opposite directions; for  $C_{18}\text{OH}$   $K_S$  becomes less favourable, while for  $C_{10}\text{OH}$   $K_S$  becomes more favourable.

For both  $C_{18}\text{GlyOH}$  and  $C_{18:1}\text{OH}$  the binding constant of the kinetic probe decreases upon the addition of alcohol, whereas at the same time the vesicular rate constant initially increases, and then decreases slightly. Although the trends for these two alcohols are similar the maximum observed rate constants are

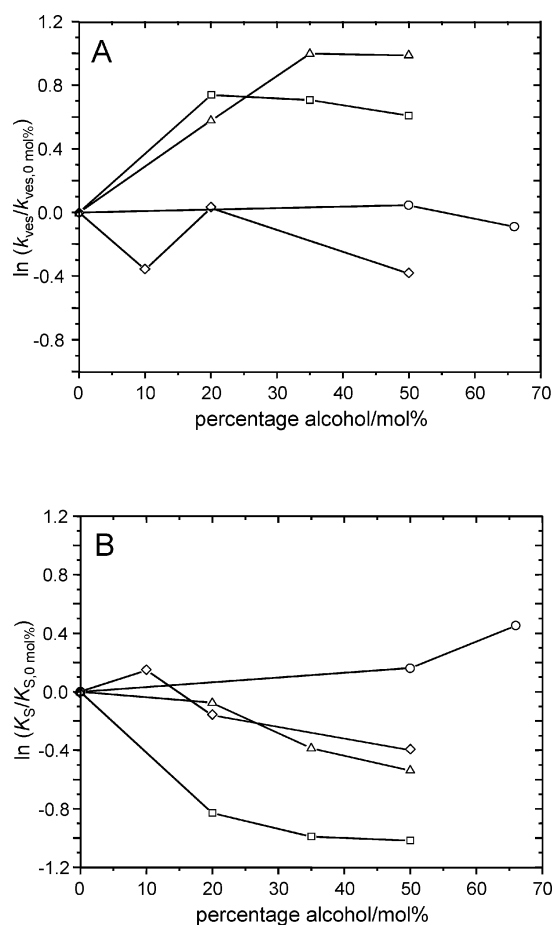


**Fig. 3** Plot of  $\ln(k_{\text{ves}}/k_{\text{ves},0} \text{ mol}\%)$  (A) and  $\ln(K_S/K_{S,0} \text{ mol}\%)$  (B) versus the mol% of the added alcohol. Fits were obtained by allowing both  $k_{\text{ves}}$  and  $K_S$  to vary. C<sub>10</sub>OH (○); C<sub>18</sub>OH (◇); C<sub>18</sub>GlyOH (□); C<sub>18:1</sub>OH (△). Lines are only drawn to guide the eye.

very different, since the extent of the increase or decrease determines whether there occurs an increase or a decrease in the maximum observed rate constant compared to the vesicles without added alcohol.

For  $S_N2$  reactions in mixed micelles of CTAB and short-tailed alcohols  $K_S$  decreases relative to CTAB micelles, whereas the micellar rate constant does not usually change.<sup>15,17–22,49</sup> The decrease in  $K_S$  can be attributed to a relative stabilisation of the kinetic probes due to the presence of the alcohols in the aqueous phase. However, in our system the concentration of alcohol in the aqueous phase is expected to be extremely low, considering the hydrophobicity of the alcohols.

We choose not to correct  $k_{\text{ves}}$  for the change in molar volume of the amphiphiles and alcohols, since molar volumes are not known for some of the alcohols used in this study. However, we stress that the molar volumes of the alcohols with 18 carbons in the chain will not be significantly different since the molar volume is mainly determined by the number of carbon atoms in the alcohol, rather than the exact structure of the molecule.<sup>49</sup>

In principle a reduced counterion binding can be used to fit our data for C<sub>10</sub>OH, C<sub>18</sub>OH and C<sub>18</sub>GlyOH, as was done for the mixed micelles of CTAB and short-tailed alcohols.<sup>15,17–22,49</sup> However, since the different alcohols would then have a different effect on the counterion binding, we anticipate that, in view of existing literature evidence, this is unlikely.<sup>50</sup> In addition, data for vesicles containing C<sub>18:1</sub>OH cannot be fitted by changing the counterion binding. Therefore it is more likely that changes in the observed rate constants mainly originate from a change in  $K_S$  and/or  $k_{\text{ves}}$ .

Also for the pyranosides only the fits using method IV will be discussed. The different results for C<sub>12</sub>Mal and C<sub>12</sub>Glu are obvious. Whereas for C<sub>12</sub>Glu the increase in the maximum

observed rate constant mainly comes from an increase in  $k_{\text{ves}}$ , for C<sub>12</sub>Mal this effect mainly originates from an increase in  $K_S$ . In fact for C<sub>12</sub>Mal  $k_{\text{ves}}$  decreases upon addition of more pyranoside. It should be noted that C<sub>10</sub>Mal is often used as a membrane solubilising agent<sup>51</sup> and that therefore our vesicles can be (partially) solubilised as well, depending on the relative amount of incorporated C<sub>12</sub>Mal. However, dynamic light scattering experiments (at 0.5 mM C<sub>18</sub>C<sub>18</sub><sup>+</sup>) show that there are still large aggregates present in solution (supplementary information †), although the decreased scattered intensity indicates that there is also significant (worm-like) micelle formation. The relative amount of amphiphile in vesicles and micelles depends on the total concentration of both amphiphile and single-tailed surfactant.

The solutions containing C<sub>12</sub>Mal behaved somewhat unusually in their macroscopic behaviour. The solutions containing 25 mol% of C<sub>12</sub>Mal became slightly turbid upon standing, but gentle shaking made the solutions transparent with a bluish colour. After about 5 min. it became turbid again. This process was repeatable. After addition of 2.25 mM NaOH from a 1 M stock solution a white precipitate was observed, which disappeared upon vigorous shaking, leading to a transparent bluish solution that was stable overnight and similar in size distribution as before NaOH addition as shown by dynamic light scattering (supplementary information †). The precipitation was also observed for solutions with 50 mol% of C<sub>12</sub>Mal. However, this solution was also very viscous, which is indicative of worm-like micelles.

These observations make the kinetic analysis more complex. The model we use only takes into account two pseudophases; an aqueous one and a vesicular one. Addition of a micellar one would lead to more variables, making it impossible to obtain any meaningful number for the fitted parameters. Therefore we do not perform this analysis quantitatively, but only qualitatively. The Kemp elimination is slower in micelles than in vesicles,<sup>52</sup> since these aggregates contain more water in their Stern region. Upon increasing amounts of C<sub>12</sub>Mal (worm-like) micelle formation increases as well (supplementary information †), and therefore the micellar rate constant will be more pronounced in the fitted value of  $k_{\text{ves}}$  at higher mole fractions of C<sub>12</sub>Mal. This effect can be seen in Fig. 4 where  $k_{\text{ves}}$  decreases again after an initial increase. This decrease is not seen for C<sub>12</sub>Glu which is not able to solubilise vesicles.

Although the (extrapolated) CMC of C<sub>12</sub>Glu (80–200 μM) has been reported,<sup>32,51,53,54</sup> we were not able to solubilise C<sub>12</sub>Glu in pure water. The binding constant of C<sub>12</sub>Glu to phosphatidylcholine membranes is estimated to be around  $2 \times 10^4 \text{ M}^{-1}$  (above 0.9 mM amphiphile more than 95% is bound).<sup>51</sup> Therefore we can safely assume that the amount of C<sub>12</sub>Glu in the aqueous phase is negligible. The CMC of C<sub>12</sub>Mal (150–200 μM) is similar to that of C<sub>12</sub>Glu.<sup>32,51,55,56</sup> However, its binding constant ( $5 \times 10^3 \text{ M}^{-1}$ ) is smaller, only leading to full binding (>95%) to the membrane above 3.5 mM amphiphile.<sup>51</sup>

The large increase in  $K_S$  for the C<sub>12</sub>Mal containing solutions is striking, whereas for C<sub>12</sub>Glu the increase in  $K_S$  amounts to only a factor of 2 after an initial decrease. Apparently, despite the structural similarity, the effect of both additives on the fitted parameters is quite different.

In the fitting procedures, specific or preferential binding of hydroxide ions to the sugar-surfactants was not taken into account. Therefore we did control experiments to see whether such binding can actually be neglected, since certain non-ionic sugar-derived surfactants are able to bind hydroxide ions.<sup>32–36</sup> In a first control experiment we compared the observed rate constants in a system with DOPC and DOPC with 25 mol% of C<sub>12</sub>Glu. As can be seen in Fig. 6 both types of vesicles show inhibition with respect to the rate constant in pure water (dashed line). As a reference we measured also the rate constant for a nonionic sugar-based gemini surfactant (GS4; Scheme 3) synthesised in our laboratory,<sup>35,36</sup> that has proven to bind

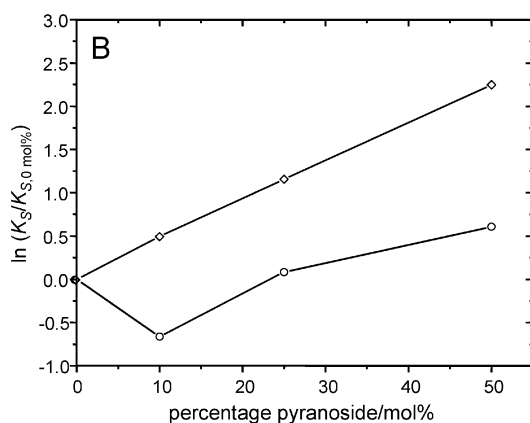
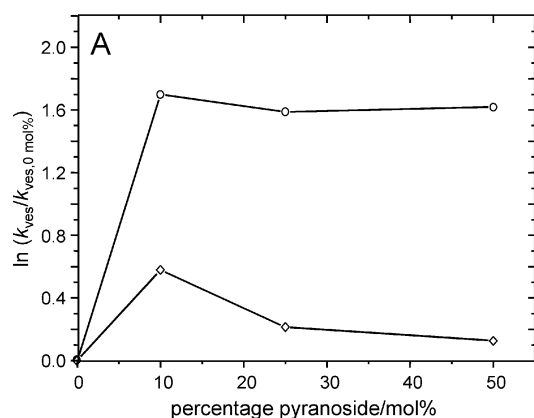


**Fig. 4** Plot of  $\ln(k_{\text{ves}}/k_{\text{ves},0\%})$  (A) and  $\ln(K_{\text{S}}/K_{\text{S},0\%})$  (B) versus the mol% of the added pyranoside. Fits were obtained by allowing both  $k_{\text{ves}}$  and  $K_{\text{S}}$  vary. C<sub>12</sub>Glu (○); C<sub>12</sub>Mal (◇). Lines are drawn to guide the eye.

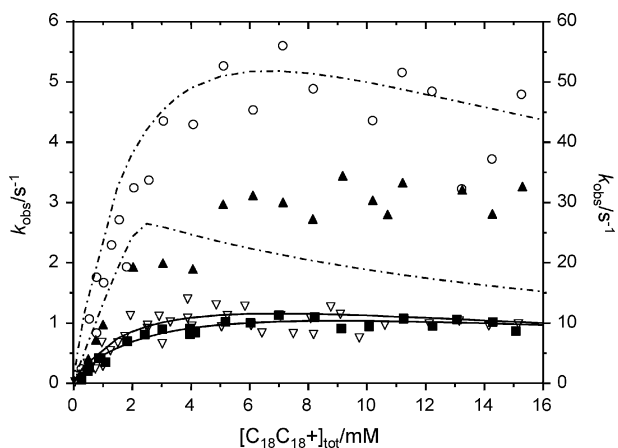


**Fig. 5** Observed rate constant of vesicles with different degrees of counterion binding with and without C<sub>12</sub>Glu. Left axis: C<sub>18</sub>C<sub>18</sub><sup>+</sup> : C<sub>10</sub>C<sub>10</sub><sup>-</sup> : C<sub>12</sub>Glu 65 : 35 : 0 (▽) and 61 : 33 : 7 (○). Right axis: 100 : 0 : 0 (■) and 90 : 0 : 10 (▲). Lines are best fits using the Langmuir isotherm of ion adsorption and a constant value for  $K_{\text{S}}$  and  $k_{\text{ves}}$ .

hydroxide ions. As can be seen, this surfactant *catalyses* the Kemp deprotonation reaction. Therefore we can exclude that there is specific hydroxide binding by C<sub>12</sub>Glu. However, it might still be possible that the presence of the sugar units in the Stern region might favour binding of hydroxide ions over the binding of chloride ions. The reasonable value we obtained for  $K_{\text{OH}}^{\text{Cl}}$  (supplementary information †) doesn't indicate such a process. However, considering that each sugar unit has five hydrogen bond donors and six acceptors, we anticipate that these might increase the binding of hydroxide ions relative to chloride through (multiple) hydrogen bonds. Therefore in a second experiment (Fig. 5) we compared four different vesicular solu-

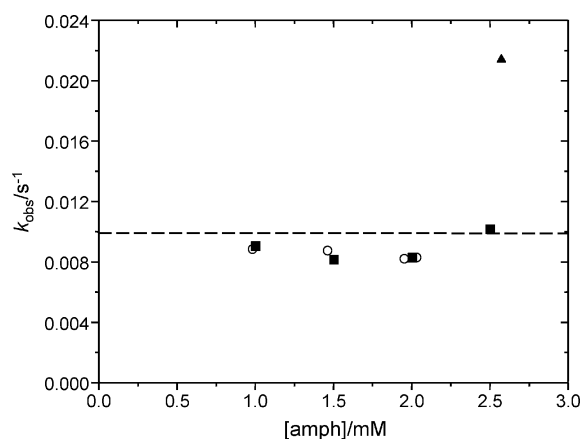
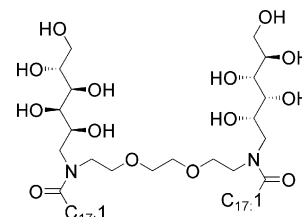


**Fig. 6** Observed rate constant for DOPC (■), DOPC with 25 mol% of C<sub>12</sub>Glu (○) and GS4<sup>35,36</sup> (▲). Dashed line represents the rate constant in water.



**Scheme 3** Structure of GS4.

tions. Solution A contained 100 mol% of C<sub>18</sub>C<sub>18</sub><sup>+</sup>, and solution B 35 mol% of C<sub>10</sub>C<sub>10</sub><sup>-</sup> (C<sub>18</sub>C<sub>18</sub><sup>+</sup> : C<sub>10</sub>C<sub>10</sub><sup>-</sup> : C<sub>12</sub>Glu = 65 : 35 : 0). The maximum observed rate constants of these solutions differ by a factor of about ten, due to a reduced counterion binding (27%) to the excess C<sub>18</sub>C<sub>18</sub><sup>+</sup> in solution B.<sup>8</sup> Then about 10 mol% of C<sub>12</sub>Glu was added to solutions A and B, which gave solutions C (90 : 0 : 10) and D (61 : 33 : 7), respectively. The maximum observed rate constants increased by a factor of 3 and 5 going from solution A to C and B to D, respectively. In an attempt to fit the data of solution C and D by only changing the counterion binding and the ion exchange constant  $K_{\text{OH}}^{\text{Cl}}$  (keeping  $K_{\text{S}}$  and  $k_{\text{ves}}$  constant) we only found a fit for solution D. It was not possible to fit the data of solution C. Not even when only hydroxide ions were considered as counterions, since there is only 2.25 mM hydroxide ions in solution. Above this concentration the two reagents are diluted within the vesicular pseudophase. In addition, in both cases the value of  $K_{\text{OH}}^{\text{Cl}}$  was just slightly above the mathematically and chemically acceptable lower limit of 1 (compare eqn. (2)). Therefore we decided to fit the data again, but use the Langmuir isotherm and mass balance to calculate the vesicular hydroxide concentration ( $m_{\text{OH}}$  eqn. (1)) instead of using eqn. (2).<sup>45</sup> The advantage is that instead of a relative binding constant for hydroxide and chloride ions,  $K_{\text{OH}}^{\text{Cl}}$ , and a fixed counterion binding  $\beta$ , the Langmuir isotherm uses separate binding constants for these ions,  $K_{\text{OH}}$  and  $K_{\text{Cl}}$ , respectively. The disadvantage is that the vesicular ion concentrations have to be calculated iteratively. For moderate salt concentrations and the presence of at least one counterion with a binding constant that is not too small, the concentration of vesicular-bound hydroxide ions in both models is comparable to that obtained from the ion exchange model,<sup>57</sup> except that the ion exchange model has a higher concentration of bound hydroxide ions at amphiphile concentrations below 2 mM.

For obvious reasons the data of solution C could still not be fitted, but it was possible to fit the data of solution D with a binding constant  $K_{\text{OH}}$  that was 7.5 times larger than that for the data of solution B.<sup>58</sup> These results indicate that preferential binding might play a role in systems containing alkyl pyranosides, but that probably additional effects play a role leading to changes in  $K_{\text{S}}$  and  $k_{\text{ves}}$  as well. This latter observation is reason-

able since the addition of linear alcohols (which are just alkyl pyranosides without the sugar part) induce changes in  $k_{\text{ves}}$  and  $K_{\text{S}}$  (*vide supra*).

### Differential scanning microcalorimetry

Differential scanning microcalorimetry was used to further characterise the modified vesicles used in the kinetic experiments. As can be seen below, all the main phase transition temperatures remained well above 15 °C, the temperature at which the kinetic experiments were performed (Fig. 7).

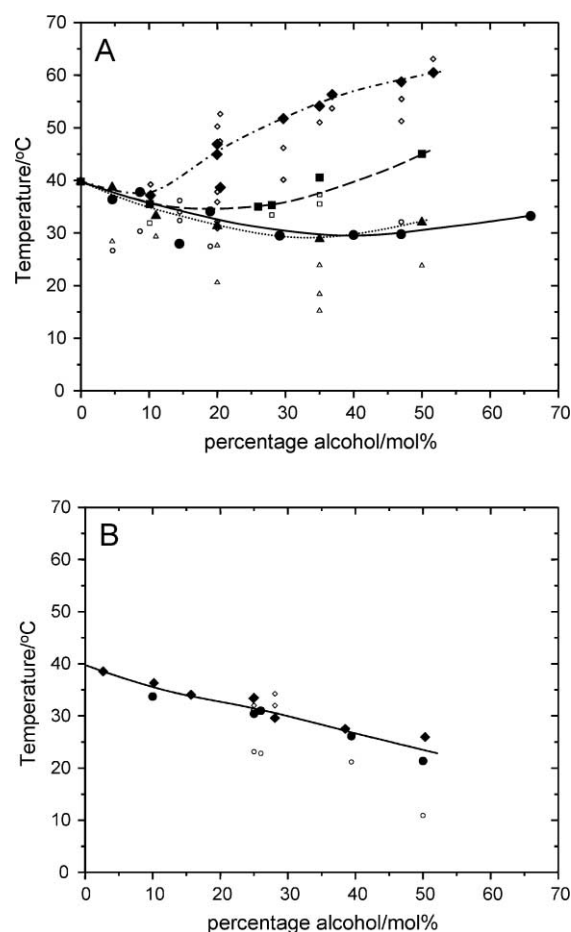


**Fig. 7** Phase transitions of  $C_{18}C_{18}^+$  vesicles with added alcohols (A) and alkyl pyranosides (B). Closed symbols are the major peak and open symbols are minor peaks. A:  $C_{10}OH$  (●);  $C_{18}OH$  (◆);  $C_{18}GlyOH$  (■);  $C_{18:1}OH$  (▲). B:  $C_{12}Glu$  (●);  $C_{12}Mal$  (◆). Lines are only drawn to guide the eye.

Addition of small amounts (<20 mol%) of saturated *n*-octadecyl alcohols to cationic vesicles of  $C_{18}C_{18}^+$  leads to a decrease of maximum 5 degrees in the main phase transition temperature. At higher mole fractions the main phase transition temperature increases, but much more rapidly and to a higher temperature for  $C_{18}OH$  than for  $C_{18}GlyOH$ . At 50 mol% the main phase transition temperature is 60 °C and 45 °C for  $C_{18}OH$  and  $C_{18}GlyOH$ , respectively. Addition of  $C_{10}OH$  leads to a decrease to 30 °C at 30 mol% and it only increases again above 50 mol% to reach a temperature of 33 °C at 66 mol%.<sup>59</sup> Addition of  $C_{18:1}OH$  leads to a similar pattern as for  $C_{10}OH$ , except that the peaks are becoming much broader (data not shown), indicating that the transition becomes much less cooperative. This is reasonable since the unsaturation in  $C_{18:1}OH$  leads to less efficient packing of the tails. These results are in agreement with literature reports where *n*-alcohols behave like amphiphiles leading to changes in the phase transition temperature that are linearly correlated with the melting point of the alcohols. This means a decrease in the phase transition temperature upon the addition of alcohols with a short ( $\leq C_8$ )

chain and an increase for alcohols with a long ( $\geq C_{12}$ ) chain.<sup>60–65</sup> Also broadening of peaks has been observed.<sup>61,62,64</sup> Experiments with linear carboxylic acids show similar trends.<sup>61,63</sup>

Finally, addition of  $C_{12}Glu$  and  $C_{12}Mal$  leads to a decrease in the main phase transition temperature. In fact, the additives can be regarded as single-tailed nonionic surfactants, especially in the case of  $C_{12}Mal$ , since the packing-parameter is lowered from >1 to  $\sim \frac{1}{3}$  with respect to linear alcohols. When single-tailed surfactants are incorporated into bilayers, due to the curvature difference with the double-tailed amphiphiles the local bilayer structure is disturbed. Since the main phase transition temperature for a great deal reflects the packing efficiency of the tails, a decrease in the main phase transition temperature is not surprising. A decrease in the main phase transition temperature was also observed for cationic vesicles with a cationic single-tailed surfactant<sup>66</sup> and for phospholipid vesicles with  $C_{12}Glu$  or  $C_{12}Mal$ .<sup>67</sup>

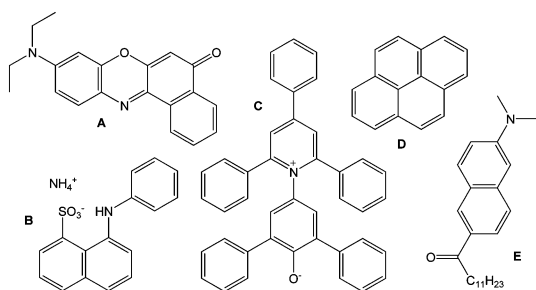
Several control experiments were performed to check the reproducibility of the DSC scans. Unfortunately, the reproducibility in certain mixtures is not too high, indicating that the vesicles are metastable and that their exact structure depends on the time between preparation and experiment, the procedure that was followed to make the vesicles, and probably some more parameters. Also, the fact that many scans show more than one peak indicates that there is either more than one transition or that the alcohol and amphiphile are not homogeneously mixed, or both. Similar effects were seen of alcohol/phospholipids mixtures.<sup>60</sup> This is especially the case for the mixtures with  $C_{18}OH$  and  $C_{18:1}OH$ , and to a much lesser extent for  $C_{10}OH$  and  $C_{18}GlyOH$ . The reason for this multiple phase formation might come from the high melting point of  $C_{18}OH$  and  $C_{18}GlyOH$ . In combination with the unfavourable packing parameter of  $C_{18}OH$  (>1), this leads to a situation where  $C_{18}OH$  dissolution in membranes of  $C_{18}C_{18}^+$  is rather unfavourable. Crystallisation of small domains rich in  $C_{18}OH$  within the membrane might occur.  $C_{18}GlyOH$  has a larger hydrophilic moiety, leading to a more favourable packing parameter and therefore it might lead to a better dissolution in the membrane making crystallisation in the membrane less favourable. The large increase in the phase transition temperature in the presence of  $C_{18}OH$  is in agreement with the observation that there is an increase in ordering in the bilayer.<sup>65</sup> Phospholipids with unsaturation in the tails usually have a phase transition temperature below 0 °C, since these unsaturations disrupt the bilayer and make efficient packing difficult. Likewise, in the dry state phospholipids with unsaturation are usually more wax-like than their saturated analogues. Therefore it is a bit surprising to notice that addition of  $C_{18:1}OH$  does not lead to a larger decrease in phase transition temperature than observed here.

The DSC heating scans for all additives are shown in the supplementary information. †

### Influence of polarity on the Kemp elimination

In order to get a better understanding of the influence of medium polarity on the rate constant of the Kemp elimination the kinetics were followed in 1,4-dioxane/water and acetonitrile/water mixtures. 1,4-Dioxane and acetonitrile were chosen since they are known to have little or no preferential solvation. Nile Red fluorescence and  $E_T(30)$  absorbance (Scheme 4 A + C) are sensitive to the polarity of the solvent or solvent mixtures.<sup>68</sup> In addition both probes are sensitive for hydrogen bonding, whereas the  $E_T(30)$  probe is more sensitive towards hydrogen bonding than Nile Red. The wavelength of maximum absorbance or fluorescence was used to calculate the normalised polarity  $P^{w/d}$  via eqn. (5):

$$P^{w/d} = \frac{\lambda_{\text{max,mixt}}^{-1} - \lambda_{\text{max,dioxane}}^{-1}}{\lambda_{\text{max,water}}^{-1} - \lambda_{\text{max,dioxane}}^{-1}} \quad (5)$$



**Scheme 4** Fluorescent probes employed: Nile Red (A), 1,8-ANS (B),  $E_T(30)$  (C), pyrene (D) and Laurdan (E).

This equation is analogous to the equation used by Reichardt to calculate the normalised  $E_T(30)$  ( $E_T^N$ ).<sup>68</sup> We normalised it in such a way that the polarity of 1,4-dioxane equals zero, and water one.

In Fig. 8 the normalised polarity was measured as a function of the water concentration by both Nile Red and Reichardt's  $E_T(30)$  probe. In the range of 56 to 20 M water Nile Red measures a polarity which does not distinguish between the use of 1,4-dioxane or acetonitrile, whereas  $E_T(30)$  reports different values for both solvents at constant water concentration. However, in Fig. 9 it can be seen that the polarity measured by  $E_T(30)$  scales linearly and independent of solvent with the natural logarithm of the observed rate constant in the solvent mixture. From the slope ( $-11.7 \pm 1.1$ ) and the intercept ( $13.2 \pm$

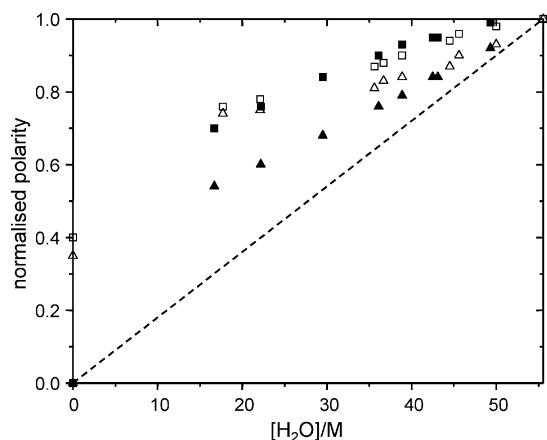


**Fig. 8** Normalised polarity as a function of water concentration in water/1,4-dioxane (closed symbols) and water/acetonitrile (open symbols) as measured by  $E_T(30)$  ( $\blacktriangle$ ) and Nile Red ( $\blacksquare$ ). The line represents linear behaviour between water concentration and normalised polarity.

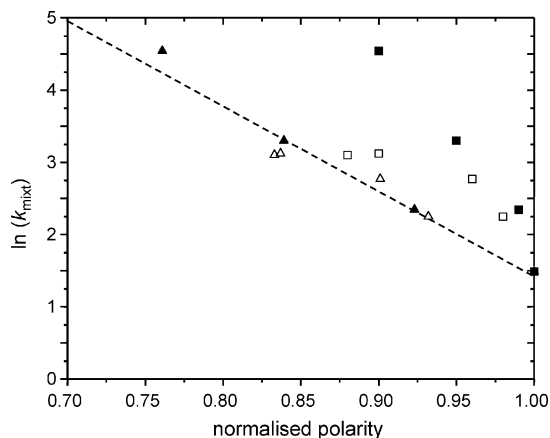


**Fig. 9** Natural logarithm of the observed rate constant for the Kemp elimination as a function of normalised polarity in water/1,4-dioxane (closed symbols) and water/acetonitrile (open symbols) as measured by  $E_T(30)$  ( $\blacktriangle$ ) and Nile Red ( $\blacksquare$ ). The line is a linear fit of the rate constant versus polarity measured by  $E_T(30)$ .

0.9) the rate constants in pure 1,4-dioxane and acetonitrile were estimated to be  $5 \times 10^5 \text{ s}^{-1}$  and  $9 \times 10^3 \text{ s}^{-1}$  respectively.

As for vesicles, the large rate increase is mainly an effect of dehydration of the reactants. Likewise, partial dehydration of the hydroxide ion is more important in the rate increase than dehydration of the kinetic probe. The linear dependence of  $\ln(k_{\text{mixt}})$  with the normalised polarity measured with  $E_T(30)$  means that the reaction is sensitive to a similar extent to polarity and hydrogen bonding as the  $E_T(30)$  probe. Therefore the  $E_T(30)$  probe was used to measure the polarity in vesicles with different amounts of alcohols and pyranosides (Fig. 10A). Unfortunately, the experiments showed to be not very reproducible. This is probably due to structural changes in the aggregate structure induced by the size and charges of the  $E_T(30)$  probe. However, the initial experiments (closed symbols) show that the polarity is not very sensitive for the composition, as is also shown by Nile Red fluorescence (Fig. 10B). The trends are independent of the excitation wavelength between 490 nm and 590 nm. For the vesicles with  $C_{12}\text{Mal}$ , or  $C_{12}\text{Glu}$  the polarity slightly decreases, whereas for  $C_{10}\text{OH}$  it slightly increases. The decrease for  $C_{12}\text{Mal}$  and  $C_{12}\text{Glu}$  could originate from a decrease in local water concentration, which would be in line with our kinetic observations.

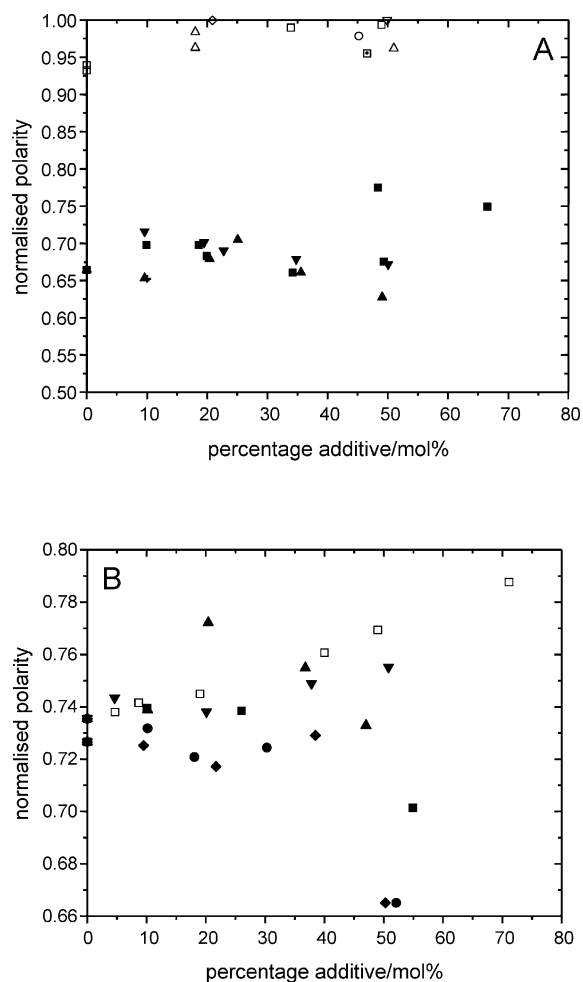


**Fig. 10** Normalised polarity as measured by  $E_T(30)$  absorbance (A) and Nile Red fluorescence (B) versus the mol% of the additive. Nile Red was excited at 590 nm. A:  $C_{10}\text{OH}$  ( $\blacksquare$ ,  $\square$ );  $C_{18}\text{OH}$  ( $\blacktriangle$ ,  $\triangle$ );  $C_{18}\text{GlyOH}$  ( $\square$ );  $C_{18:1}\text{OH}$  ( $\blacktriangledown$ );  $C_{12}\text{Glu}$  ( $\circ$ );  $C_{12}\text{Mal}$  ( $\diamond$ ). B:  $C_{10}\text{OH}$  ( $\square$ );  $C_{18}\text{OH}$  ( $\blacktriangle$ );  $C_{18}\text{GlyOH}$  ( $\blacksquare$ );  $C_{18:1}\text{OH}$  ( $\blacktriangledown$ );  $C_{12}\text{Glu}$  ( $\bullet$ );  $C_{12}\text{Mal}$  ( $\blacklozenge$ ).

To further characterise the polarity of the bilayer we employed the fluorescent dyes ANS, Laurdan and pyrene (Scheme 4 B + D + E; supplementary information<sup>†</sup>). ANS is sensitive towards changes in polarity of the Stern region,<sup>69,70</sup> showing a blue shift in the fluorescence maximum upon a



polarity decrease of the Stern region. In water the fluorescence is quenched. This quenching is absent for pyrene, since it does not contain a hydrogen-bond accepting or donating group. Pyrene senses a change in polarity *via* a relative change in the intensity of the first and third vibronic peak in the spectrum. The ratio of the first and third peak can be used as a measure of polarity.<sup>71</sup> Laurdan fluorescence is sensitive for the phase of the tails *via* the relative intensity of the two peaks that are observed in the emission spectrum.<sup>72</sup> Below the phase transition temperature the peak at lower wavelength is larger than the peak at higher wavelengths leading to a positive value for GP (generalised polarisation). Above the phase transition temperature the relative intensity is inverted, leading to a negative value for GP.

In vesicles containing alcohols and pyranosides the GP value is positive and no significant change in the value is observed (supplementary information). Also pyrene and ANS fluorescence (supplementary information) show no significant change upon the addition of alcohols or pyranosides.

### Consequences for the kinetic analysis

All kinetic experiments were performed at 15 °C, which is well below the main phase transition temperature of the vesicles with additives (*vide supra*). This is confirmed by the constant positive GP value as sensed by Laurdan. The experiments performed to reveal the change in (normalised) polarity in the bilayer upon the addition of linear alcohols and alkyl pyranosides show that the polarity changes only slightly. The slight changes are fluorescent- and absorbance-dye dependent. This is reasonable since the probes are sensitive towards different intermolecular interactions. For example, the  $E_T(30)$  dye is particularly sensitive towards hydrogen-bond donation, whereas pyrene is not. The differences between the fitted parameters for the alcohols are relatively small, although the differences between the observed rate constants are more pronounced. In addition, parameter compensation has to be taken into account. Despite these mathematical consequences, the small changes in the fitted parameters are in agreement with the small changes in the measured normalised polarity.

Strikingly, the changes in  $k_{\text{ves}}$  and  $K_S$  for vesicular solutions containing alkyl pyranosides are not apparent from the changes in measured normalised polarity, or by a transition of the tails from gel-like to liquid-crystalline. Since the vesicular rate constant scales with the normalised polarity, the vesicular rate constant should not change too much. However, nonionic micelles containing  $C_{12}\text{Mal}$  or  $C_{12}\text{Glu}$  have an interface that is “aqueous-like” in nature,<sup>55</sup> *i.e.* the effective dielectric constant is larger than that for nonionic micelles with an oligo-ethylene oxide head group.  $C_{12}\text{Glu}$  and  $C_{12}\text{Mal}$  retain their hydration cospheres, and as a result, anions present in the same region are less hydrated similar to what was observed for mixed micelles of CTAB and a nonionic cosurfactant,<sup>21,22</sup> leading to an increase in  $k_{\text{ves}}$ .<sup>39–41</sup> This observation is also found for mixed micelles of SDS and dodecylmalono-bis-*N*-methylglucamide. Below a mole fraction SDS of 0.3 the head group region is completely dehydrated, since the sugar units have replaced all the water molecules in the interfacial region.<sup>31</sup> However, at this stage the counterion binding is still about 40%. The probes used to measure the local polarity are not sensitive towards these changes, and hence they report a constant polarity upon increasing amounts of  $C_{12}\text{Mal}$  and  $C_{12}\text{Glu}$ . In the organic solvent/water mixtures a change in dehydration of the hydroxide ion is automatically coupled to a change in polarity.

Based on these observations, it seems reasonable to assume that the hydroxide ions in the Stern region of vesicles formed from  $C_{18}C_{18}^+$  in the presence of  $C_{12}\text{Mal}$  or  $C_{12}\text{Glu}$  are more dehydrated compared to vesicles with no alkyl pyranosides. This increases the reactivity of the hydroxide ion and in

turn  $k_{\text{ves}}$  increases without the normalised polarity changing significantly. Finally, we note that the decrease in  $k_{\text{ves}}$  above 10 mol% of  $C_{12}\text{Mal}$  is probably due to micelle-formation.<sup>52</sup>

### Conclusions

Cationic vesicles of  $C_{18}C_{18}^+$  catalyse the Kemp elimination *ca.* 50 times relative to the second-order rate constant in water.<sup>8</sup> This effect is mainly attributed to a change in polarity going from water to the aqueous pseudophase, where partial dehydration of the hydroxide ion is the main contribution to the rate enhancement.

The observed catalysis of the Kemp elimination is decreased upon the addition of  $C_{10}\text{OH}$ ,  $C_{18}\text{OH}$  and  $C_{18}\text{GlyOH}$  to the  $C_{18}C_{18}^+$  vesicles, although the extent of the decrease depends on the exact structure of the additive. By contrast, the catalysis is increased upon the addition of  $C_{18:1}\text{OH}$ ,  $C_{12}\text{Mal}$  and  $C_{12}\text{Glu}$ , reaching a maximum at 35 mol% of  $C_{18:1}\text{OH}$ . No maximum is reached in the observed catalysis up to 50 mol% of  $C_{12}\text{Glu}$  and  $C_{12}\text{Mal}$ . The data can be fitted using a decreasing counterion binding with increasing additive content and an ion exchange constant fixed at 1.6, leading to realistic values for  $k_{\text{ves}}$  and  $K_S$ . The analysis shows that for  $C_{10}\text{OH}$ ,  $C_{18}\text{OH}$  and  $C_{18:1}\text{OH}$ ,  $k_{\text{ves}}$  and  $K_S$  only change slightly (at most a factor of around two). For  $C_{18}\text{GlyOH}$ ,  $C_{12}\text{Glu}$  and  $C_{12}\text{Mal}$ , the situation is different. The vesicular rate constant in  $C_{18}C_{18}^+$  vesicles with  $C_{18}\text{GlyOH}$  is over a factor of two larger than in the absence of additive, whereas  $C_{12}\text{Glu}$  has a  $k_{\text{ves}}$  that is 5 times higher. At low mole percentage,  $C_{12}\text{Mal}$  also shows an increase in  $k_{\text{ves}}$ , but due to the formation of (worm-like) micelles  $k_{\text{ves}}$  decreases again. The binding constant in vesicles with  $C_{18}\text{GlyOH}$  decreases, whereas for 50 mol% of  $C_{12}\text{Mal}$   $K_S$  is almost ten fold larger. After a decrease of  $K_S$  in  $C_{18}C_{18}^+$  vesicles with a low  $C_{12}\text{Glu}$  content, an increase is also observed at higher  $C_{12}\text{Glu}$  content.

The main phase transition temperatures for the mixtures were measured with differential scanning microcalorimetry. All alcohols showed initially a decrease in the main phase transition temperature, and then, above a certain mole fraction an increase. The extent of the increase or decrease depends on both the structure of the additive and the amount that is present in the bilayer. Addition of alkyl pyranosides leads to a linear decrease of the phase transition temperature with about 15 °C at 50 mol% alkyl pyranoside.

The natural logarithm of the rate constant of the Kemp elimination shows a linear increase with a decreasing  $E_T(30)$  value in water/1,4-dioxane and water/acetonitrile mixtures. Nile Red fluorescence is not linearly related to the natural logarithm of the rate constant. However, Nile Red is not as sensitive as  $E_T(30)$  to hydrogen bonding, indicating that hydrogen bonding plays a major role in the reaction. The large increase in  $k_{\text{ves}}$  for  $C_{12}\text{Glu}$ , without a significant change in the measured normalised polarity, as measured by  $E_T(30)$ , Nile Red, ANS, pyrene and Laurdan, indicates that the hydroxide ion is more dehydrated than when the alkyl pyranosides are absent. This observation is consistent with literature evidence that sugar-based surfactants dehydrate the interfacial region, without destroying its “aqueous-like” nature.

The complex change in observed rate constants as a function of the structure of the additives on the catalysis of the Kemp elimination indicates that subtle changes in the structure of the additive can lead to significant changes in the interfacial structure of vesicles. However, these changes do not originate from a change in polarity, indicating that other factors (*e.g.* water concentration, bilayer packing, domain formation *etc.*) play a more important role. This is further exemplified by the large dependence of the DSC scans on the structure and concentration of the additive. Unfortunately, the exact molecular nature of these changes of the properties of vesicles is experimentally difficult to determine. If the observations

described in this paper are translated to biological membranes it seems clear that subtle changes in the structure and relative amounts of the lipids, steroids and proteins will strongly influence the interfacial properties of biological membranes and, consequently, reactions occurring at this interface. Special attention should be paid to glycolipids since they seem to have unexpected behaviour on the interfacial properties.

## Experimental

### Materials

Dimethyldi-*n*-octadecylammonium chloride (>97%; Fluka), *n*-decanol (99%; Aldrich), *n*-octadecanol (95%; Acros), oleyl alcohol (Aldrich), batyl alcohol (99%; Aldrich), *n*-dodecyl- $\beta$ -glucoside (>99%; Fluka), *n*-dodecyl- $\beta$ -maltoside (>99.5%; Glycon), sodium hydroxide (titrisol; Merck), pyrene (>99%; Aldrich), 8-anilino-1-naphthalenesulfonic acid ammonium salt (ANS; Sigma), 6-dodecanol-2-dimethylaminonaphthalene (Laurdan; >99%; Molecular Probes), 9-diethylamino-5*H*-benzo[*a*]phenoxazine-5-one (Nile Red; 99%; Acros), sodium hydroxide (Titrisol) and dioleoylphosphatidylcholine (DOPC; 99%; Avanti) were used as received. The  $E_T(30)$ -probe (2,6-diphenyl-4-(2,4,6-triphenyl-1-pyridinio)phenolate) was kindly provided by Prof. Ch. Reichardt (University of Marburg). 5-Nitrobenzisoxazole (**1**) was a generous gift from Dr. F. Hollfelder and Prof. A.J. Kirby of the University Chemical Laboratory (Cambridge, UK). GS4 and sodium didecylphosphate were synthesized as described previously.<sup>36,73</sup> Doubly distilled water was used for all solutions.

### Measurements

Vesicles were prepared as described before,<sup>8</sup> using two different procedures. In the first procedure amphiphile and additive were cosonicated in water. In the second procedure amphiphile and additive were homogeneously dissolved in a small amount of chloroform, followed by removal of the organic solvent under a stream of nitrogen and subsequent removal of residual organic solvent under vacuum. Then the film was hydrated and sonicated. Both procedures end with several extrusions of the transparent bluish solutions through a membrane with a pore size of 200 or 400 nm. In all cases the obtained vesicles have a size of around 80 to 100 nm (data not shown) unless stated otherwise.

Kinetic experiments, DSC scans,  $E_T(30)$  measurements and pyrene fluorescence were performed as described before.<sup>8</sup> Nile Red and 1,8-ANS fluorescence experiments were performed in a similar way as pyrene fluorescence except that the excitation wavelength was changed to 490 nm and 590 nm for Nile Red and 380 nm for 1,8 ANS. The wavelength of maximum fluorescence was fitted from a scan with a step size of 4 nm starting well before and ending well after the peak. Laurdan emission spectra were recorded as a function of the excitation at 440 nm and 490 nm. The recorded peaks were deconvoluted and the intensities from the fit were used to calculate the GP value:

$$GP_{440\text{ or }490} = \frac{I_{\text{blue,exc}} - I_{\text{red,exc}}}{I_{\text{blue,exc}} + I_{\text{red,exc}}} \quad (6)$$

in which  $I_{\text{blue,exc}}$  and  $I_{\text{red,exc}}$  are the fitted intensities of the peak on the blue and red side of the spectrum, respectively.

All experiments were performed at  $15.0 \pm 0.1$  °C.

It is assumed that the Kemp elimination reaction takes place both at the inner and outer leaflet of the vesicles with equal rate constants, since hydroxide ions are known to cross the bilayer fast on the time scale of the reaction (and therefore OH<sup>-</sup> crossing is not the rate-limiting step).<sup>74-77</sup> This is in agreement with observations in the literature on kinetics in solutions

containing C<sub>18</sub>C<sub>18</sub><sup>+</sup>.<sup>6,78</sup> Different rate constants have been found for the endo- and exovesicular leaflet for other reactions.<sup>79,80</sup> Distribution of **1** is considered to be fast since **1** is small, hydrophobic and nonionic.

## Acknowledgements

The National Research School Combination Catalysis is acknowledged for financial support. Mr A. Wagenaar is thanked for the synthesis of sodium didecylphosphate and GS4. Markus Johnsson and Theo Rispen are thanked for fruitful discussions.

## References

- I. V. Berezin, K. Martinek and A. K. Yatsimirskii, *Russ. Chem. Rev. (Engl. Transl.)*, 1973, **42**, 787–802.
- C. A. Bunton, F. Nome, F. H. Quina and L. S. Romsted, *Acc. Chem. Res.*, 1991, **24**, 357–364.
- P. A. Grieco, *Organic Synthesis in Water*, Thomson Science, London, 1998.
- S. Otto and J. B. F. N. Engberts, *Pure Appl. Chem.*, 2000, **72**, 1365–1372.
- I. M. Cuccovia, M. K. Kawamuro, M. A. K. Krutman and H. Chaimovich, *J. Am. Chem. Soc.*, 1989, **111**, 365–366.
- P. Hervés, J. R. Leis, J. C. Mejuto and J. Pérez-Juste, *Langmuir*, 1997, **13**, 6633–6637.
- T. Rispen and J. B. F. N. Engberts, *Org. Lett.*, 2001, **3**, 941–943.
- J. E. Klijn and J. B. F. N. Engberts, *J. Am. Chem. Soc.*, 2003, **125**, 1825–1833.
- F. M. Menger and C. E. Portnoy, *J. Am. Chem. Soc.*, 1967, **89**, 4698–4703.
- R. A. Mackay and C. Hermansky, *J. Phys. Chem.*, 1981, **85**, 739–744.
- V. Athanassakis, C. A. Bunton and F. De Buzzaccarini, *J. Phys. Chem.*, 1982, **86**, 5003–5009.
- C. A. Bunton and F. De Buzzaccarini, *J. Phys. Chem.*, 1982, **86**, 5010–5014.
- V. Athanassakis, C. A. Bunton and D. C. McKenzie, *J. Phys. Chem.*, 1986, **90**, 5858–5862.
- C. Otero and E. Rodenas, *J. Phys. Chem.*, 1986, **90**, 5771–5775.
- C. R. A. Bertoncini, F. Nome, G. Cerichelli and C. A. Bunton, *J. Phys. Chem.*, 1990, **94**, 5875–5878.
- C. R. A. Bertoncini, M. D. S. Neves, F. Nome and C. A. Bunton, *Langmuir*, 1993, **9**, 1274–1279.
- M. Muñoz, A. Rodríguez, M. D. M. Graciani and M. L. Moyá, *Langmuir*, 1999, **15**, 1588–1590.
- A. Rodríguez, M. Muñoz, M. D. M. Graciani and M. L. Moyá, *J. Colloid Interface Sci.*, 2002, **248**, 455–461.
- M. Muñoz, M. D. M. Graciani, A. Rodríguez and M. L. Moyá, *J. Colloid Interface Sci.*, 2003, **266**, 208–214.
- C. A. Bunton, S. Wright, P. M. Holland and F. Nome, *Langmuir*, 1993, **9**, 117–120.
- A. Blaskó, C. A. Bunton, E. A. Toledo, P. M. Holland and F. Nome, *J. Chem. Soc., Perkin Trans. 2*, 1995, 2367–2373.
- H. J. Forudian, C. A. Bunton, P. M. Holland and F. Nome, *J. Chem. Soc., Perkin Trans. 2*, 1996, 557–561.
- M. N. Khan, E. Ismail and M. R. Yusoff, *J. Phys. Org. Chem.*, 2001, **14**, 669–676.
- M. N. Khan and E. Ismail, *J. Phys. Org. Chem.*, 2002, **15**, 374–384.
- www.avantilipids.com/NaturalProducts.html.
- F. Paltauf, *Chem. Phys. Lipids*, 1994, **74**, 101–139.
- A. A. Farooqui, L. A. Horrocks and T. Farooqui, *Chem. Phys. Lipids*, 2000, **106**, 1–29.
- E. A. Dawidowicz, *Ann. Rev. Biochem.*, 1987, **56**, 43–57.
- C. Stubenrauch, *Curr. Opin. Colloid Interface Sci.*, 2001, **6**, 160–170.
- B. Alberts, D. Bray, J. Lewis, M. Raff, K. Roberts and J. D. Watson, in *Molecular Biology of the Cell*, Garland Publishing, New York, 1994, pp. 477–485.
- P. C. Griffiths, E. Pettersson, P. Stilbs, A. Y. F. Cheung, A. M. Howe and A. R. Pitt, *Langmuir*, 2001, **17**, 7178–7181.
- D. Balzer, *Langmuir*, 1993, **9**, 3375–3384.
- T. Baba, L. Q. Zheng, H. Minamikawa and M. Hato, *J. Colloid Interface Sci.*, 2000, **223**, 235–243.
- L. Q. Zheng, L. L. Shui, Q. Shen, G. Z. Li, T. Baba, H. Minamikawa and M. Hato, *Colloids Surf. A*, 2002, **207**, 215–221.
- M. Johnsson, A. Wagenaar and J. B. F. N. Engberts, *J. Am. Chem. Soc.*, 2003, **125**, 757–760.

- 36 M. Johnsson, A. Wagenaar, M. C. A. Stuart and J. B. F. N. Engberts, *Langmuir*, 2003, **19**, 4609–4618.
- 37 K. G. Marinova, R. G. Alargova, N. D. Denkov, O. D. Velez, D. N. Petsev, I. B. Ivanov and R. P. Borwankar, *Langmuir*, 1996, **12**, 2045–2051.
- 38 M. L. Casey, D. S. Kemp, K. G. Paul and D. D. Cox, *J. Org. Chem.*, 1973, **38**, 2294–2301.
- 39 M. Henchman, J. F. Paulson and P. M. Hierl, *J. Am. Chem. Soc.*, 1983, **105**, 5509–5510.
- 40 K. Tanaka, G. I. Mackay, J. D. Payzant and D. K. Bohme, *Can. J. Chem.*, 1976, **54**, 1643–1659.
- 41 M. J. S. Dewar and D. M. Storch, *Chem. Commun.*, 1985, 94–96.
- 42 L. S. Romsted, in *Micellization, Solubilization and Microemulsions*, K. L. Mittal, ed. Plenum Press, New York, 1977, pp. 509–530.
- 43 H. Al-Lohedan, C. A. Bunton and L. S. Romsted, *J. Phys. Chem.*, 1981, **85**, 2123–2129.
- 44 H. Al-Lohedan and C. A. Bunton, *J. Org. Chem.*, 1982, **47**, 1166–1171.
- 45 E. Rodenas and S. Vera, *J. Phys. Chem.*, 1985, **89**, 513–516.
- 46 C. A. Bunton and A. Cuenca, *Can. J. Chem.*, 1986, **64**, 1179–1183.
- 47 T. J. Broxton, J. R. Christie and X. Sango, *J. Org. Chem.*, 1987, **52**, 4814–4817.
- 48 M. N. Khan and E. Ismail, *J. Chem. Soc., Perkin Trans. 2*, 2001, **8**, 1346–1350.
- 49 C. Bravo, J. R. Leis and M. E. Peña, *J. Phys. Chem.*, 1992, **96**, 1957–1961.
- 50 J. F. Rathman and J. F. Scamehorn, *J. Phys. Chem.*, 1984, **88**, 5807–5816.
- 51 H. Heerklotz and J. Seelig, *Biochim. Biophys. Acta*, 2000, **1508**, 69–85.
- 52 J. Pérez-Juste, F. Hollfelder, A. J. Kirby and J. B. F. N. Engberts, *Org. Lett.*, 2000, **2**, 127–130.
- 53 K. Shinoda, T. Yamaguchi and R. Hori, *Bull. Chem. Soc. Jpn.*, 1961, **34**, 237–241.
- 54 Antrace Catalogue.
- 55 C. J. Drummond, G. G. Warr, F. Grieser, B. Ninham and D. F. Evans, *J. Phys. Chem.*, 1985, **89**, 2103–2109.
- 56 U. Kragh-Hansen, M. le Maire and J. V. Møller, *Biophys. J.*, 1998, **75**, 2932–2946.
- 57 M. D. M. Graciani, A. Rodríguez, M. Muñoz and M. L. Moyá, *Langmuir*, 2002, **18**, 3476–3481.
- 58 For solutions A to D we used  $K_{OH} = 380, 70, 5 \times 10^5, 525 \text{ M}^{-1}$ , respectively.  $K_{Cl}$  was kept constant at  $494 \text{ M}^{-1}$ .
- 59 H. Kamaya, N. Matubayasi and I. Ueda, *J. Phys. Chem.*, 1984, **88**, 797–800.
- 60 F. K. Hui and P. G. Barton, *Biochim. Biophys. Acta*, 1973, **296**, 510–517.
- 61 A. W. Eliaz, D. Chapman and D. F. Ewing, *Biochim. Biophys. Acta*, 1976, **448**, 220–230.
- 62 G. B. Zavoico, *Biochemistry*, 1976, **15**, 2448–2454.
- 63 S. Mabrey and J. M. Sturtevant, *Biochim. Biophys. Acta*, 1977, **486**, 444–450.
- 64 M. K. Jain and N. M. Wu, *J. Membr. Biol.*, 1977, **34**, 157–201.
- 65 G. B. Zavoico, L. Chandler and H. Kutchai, *Biochim. Biophys. Acta*, 1985, **812**, 299–312.
- 66 M. J. Blandamer, B. Briggs, P. M. Cullis, J. B. F. N. Engberts and A. Kacperska, *J. Chem. Soc., Faraday Trans.*, 1995, **91**, 4275–4278.
- 67 B. Carion-Taravella, S. Lesieur, J. Chopineau, P. Lesieur and M. Ollivon, *Langmuir*, 2002, **18**, 325–335.
- 68 C. Reichardt, *Chem. Rev.*, 1994, **94**, 2319–2358.
- 69 J. Slavik, *Biochim. Biophys. Acta*, 1982, **694**, 1–25.
- 70 L. A. M. Rupert, J. B. F. N. Engberts and D. Hoekstra, *J. Am. Chem. Soc.*, 1986, **108**, 3920–3925.
- 71 K. Kalyanasundaram and J. K. Thomas, *J. Am. Chem. Soc.*, 1977, **99**, 2039–2044.
- 72 T. Parasassi, G. Destasio, A. Dubaldo and E. Gratton, *Biophys. J.*, 1990, **57**, 1179–1186.
- 73 A. Wagenaar, L. A. M. Rupert, J. B. F. N. Engberts and D. Hoekstra, *J. Org. Chem.*, 1989, **54**, 2638–2642.
- 74 C. D. Tran, P. L. Klahn, A. Romero and J. H. Fendler, *J. Am. Chem. Soc.*, 1978, **100**, 1622–1624.
- 75 J. W. Nichols and D. W. Deamer, *Proc. Natl. Acad. Sci. USA*, 1980, **77**, 2038–2042.
- 76 S. Kaiser and H. Hoffmann, *J. Colloid Interface Sci.*, 1996, **184**, 1–10.
- 77 K. Kachel, E. Asuncion-Punzalan and E. London, *Biochim. Biophys. Acta*, 1998, **1374**, 63–76.
- 78 J. H. Fendler and W. L. Hinze, *J. Am. Chem. Soc.*, 1981, **103**, 5439–5447.
- 79 R. A. Moss and S. Swarup, *J. Org. Chem.*, 1988, **53**, 5860–5866.
- 80 R. A. Moss, S. Bhattacharya and S. Chatterjee, *J. Am. Chem. Soc.*, 1989, **111**, 3680–3687.